

Variable Flip Angle MR Imaging of 3He Spin Lattice Relaxation Times for Measurement of Alveolar Oxygen Partial Pressure

A. V. Ouriadov¹, A. Evans¹, W. Lam¹, R. Etemad-Rezai², G. Parraga¹, D. McCormack³, and G. Santyr¹

¹Imaging Research Laboratories, Robarts Research Institute, London, Ontario, Canada, ²Department of Radiology and Nuclear Medicine, London Health Science Centre, London, Ontario, Canada, ³Department of Respiratory, Department of Medicine, London Health Science Centre, London, Ontario, Canada

INTRODUCTION: Measurement of the spin-lattice relaxation time of helium due to oxygen in the lung (T_{1,O_2}) has been proposed as a method for estimation of the regional alveolar oxygen partial pressure, p_{A,O_2} (1). In diseased animals, where ventilation and perfusion can be strongly impaired, regional variations in p_{A,O_2} are expected and can be used to compute ventilation/perfusion mismatch (2). However, measurement of T_{1,O_2} using hyperpolarized gases is complicated by the cumulative effects of RF pulses ('history'), leading to image blurring. Variable flip angle (VFA) pulse sequences are less sensitive to RF pulse history and therefore may provide a more robust method for multislice mapping of p_{A,O_2} . In this work, a VFA approach is described theoretically and tested experimentally in rats and compared to results obtained using the traditional constant flip angle (CFA) RF pulse method. The feasibility of the VFA technique is also demonstrated in normal human subjects. The results confirm that the VFA technique can reduce image blurring and provide more accurate p_{A,O_2} estimates.

THEORY: Including the effects of T_1 (4), the MR signal strength of the VFA method (5) can be written as:

$$S_N = \text{const} \cdot \sin(\alpha_N) \exp\left(-\frac{1}{\xi} \int_0^t p_{A,O_2}(t) dt\right); \quad \alpha_N = \tan^{-1}\left[\frac{1}{\sqrt{N-1}}\right] \quad [1]$$

where ξ is the inverse T_1 relaxivity of oxygen (≈ 2.6 bar s), N is a total number of VFA pulses and $N \times TR \ll T_1$. Fig. 1 shows a comparison of simulated VFA versus CFA T_1 estimates. This figure was generated by analysis of simulated images in which Gaussian T_1 distributions were randomly seeded. The CFA technique is seen to result in image blurring due to the RF pulse history, and this appears to lead to a systematic underestimation of T_1 compared to the VFA technique as can be seen by the deviation from the line of identity.

METHODS: Helium MR imaging was performed at 3T (GEHC, Excite 12.0) corresponding to a helium frequency of 97.32 MHz. A commercial, rat-sized quadrature birdcage coil (Morris Instruments Inc., Ottawa, ON) and a home-built insert gradient set with maximum gradient values of 50 G/cm optimized for rodents were employed for rat imaging measurements.

Clinical whole-body gradients and a commercial, rigid elliptical chest RF coil (Rapid Biomedical, Würzburg, Germany) was used for human measurements. Hyperpolarized helium (polarization $\sim 35\%$) was provided by a turn-key spin-exchange polarizing system (Helispin[®], GEHC). The gas was administered using a custom ventilator. (GEHC), including non-magnetic valve assembly for delivery of helium within the MR environment with minimal depolarization (6)

Helium MR imaging was performed on six Wistar rats (400-450 g) following an animal care protocol approved by the University of Western Ontario. Hyperpolarized helium (polarization $\sim 35\%$) images were obtained in the coronal plane using a fast gradient-echo FGRE method with both CFA and VFA approaches and centric k-space sampling (TE=0.5 ms, TR=2.3 ms, 5 x 5 cm, 128 x 128 pixels, 22 slices of thickness 2 mm each) triggered by the ventilator. Two data sets were acquired sequentially with 50 ms separation time. The total acquisition time for each data set was 9.5 s (ie. a total breath-hold interval of 19 s). The total number of RF pulses applied for the acquisition of both data sets was $N = 5632$. T_1 maps were calculated by fitting the two data sets of the central slice with an exponential decay curve on a pixel-by-pixel basis. The rats were prepared with one, two, and three wash-out helium breaths prior to T_1 measurement in order to vary the oxygen concentrations in the rat lungs.

Five healthy volunteers were imaged following a protocol approved by the UWO Standing Board of Human Research Ethics. Two 14-slice, 2D FGRE VFA acquisitions with 7 seconds delay between each were obtained in the coronal plane during one breath-hold (14 sec) of helium following normal breathing of room air. FOV was 40 x 40 cm, matrix was 128 x 128, TE was 1.1 ms and TR was 4.6 ms. Slice thickness was 1.5 cm. For calculation of p_{A,O_2} , the two images were analyzed on a pixel-by-pixel basis using Eqn. 1.

RESULTS: Mean T_1 values and standard deviations obtained by VFA and CFA techniques in the rats are compared in Table 1. In this Table, mean values represent the average values over the whole T_1 map. Whereas no significant change in CFA T_1 values was observed with varying number of wash-out breaths, the VFA method demonstrates the expected gradual increase in mean T_1 values with decreasing p_{A,O_2} concentrations due to the wash-out breaths. The insensitivity of CFA to changes in oxygenation is consistent with the simulations (Fig. 1) and presumably arises from image blurring that leads to under-estimation of T_1 . Although the T_1 values were likely changing due to the oxygen depletion rate (ODR) by the tissue during the 19 second measurement time, the extracted average T_1 values reflect a time-averaged p_{A,O_2} that follows the expected trend. Table 2 shows the VFA T_1 and p_{A,O_2} results from the normal human subjects. These values are approximately those expected following normal breathing of room air and are consistent with the rat results. Figs. 2a and b show typical T_1 maps obtained with the VFA technique from rat and human lungs respectively.

Table 1: T_1 values and standard deviations in rat lung

	one wash-out breath		two wash-out breaths		three wash-out breaths	
	$\langle T_1 \rangle$, s	σ	$\langle T_1 \rangle$, s	σ	$\langle T_1 \rangle$, s	σ
CFA	15.09	7.86	15.53	7.10	15.09	7.86
VFA	29.44	18.53	38.32	27.68	29.44	18.53

Table 2: T_1 , p_{A,O_2} values and standard deviations for human subjects

	1		2		3		4		5	
	mean	σ	mean	σ	mean	σ	mean	σ	mean	σ
T_1	8.7	1.8	12.8	5.1	13.7	7.8	17.1	9.2	9.3	3.2
p_{A,O_2}	0.31	0.07	0.23	0.09	0.22	0.1	0.19	0.11	0.30	0.09

DISCUSSION: The VFA method provides a measure of p_{A,O_2} without the blurring due to RF pulse history associated with CFA methods. This blurring appears to cause an apparent underestimation of T_1 and corresponding overestimation of p_{A,O_2} . The clinical and preclinical VFA results are in good agreement. It is interesting to point out that it is expected that significant T_1 decay during image acquisition will also lead to blurring when $N \times TR \sim T_1$ in Eq. [1] which may also overestimate p_{A,O_2} . Particularly, to adequately sample short T_1 decay, with long image acquisition times (ie. 3D), this blurring may be mitigated using a VFA pulse sequence (Eqn. 1) which accounts for signal decay due to both RF pulse history and T_1 decay during image acquisition. This will further improve the accuracy of T_1 (and p_{A,O_2}) estimates.

REFERENCES:

1. Moller, et al. MRM 2001;45:421-30.
2. Fischer, ISMRM 2005, 1818.
3. Wild, et al. ISMRM 2005, 1805.
4. Deninger, et al. MRM 2002;47:105-14.
5. Zhao, et al. J. Magn. Reson. B 1996;113:179-183.
6. Deninger, et al. MRM 2002;48:223-32.

ACKNOWLEDGEMENTS: This work was supported in part by the Ontario Thoracic Society, Canadian Institutes of Health Research and Merck. The helium polarizer was made available by Merck and GEHC. Thanks to M. Nicole Hague and Heather Anne Cadieux for assistance with animal care. Thanks also to Cyndi Harper-Little, Shayna McKay, Christine Piechowicz and Sandra Halko for assistance with human subjects.

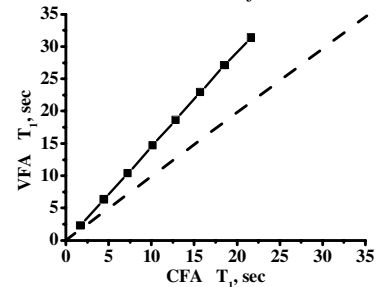


Fig 1. Simulated T_1 estimates using VFA versus CFA approaches.

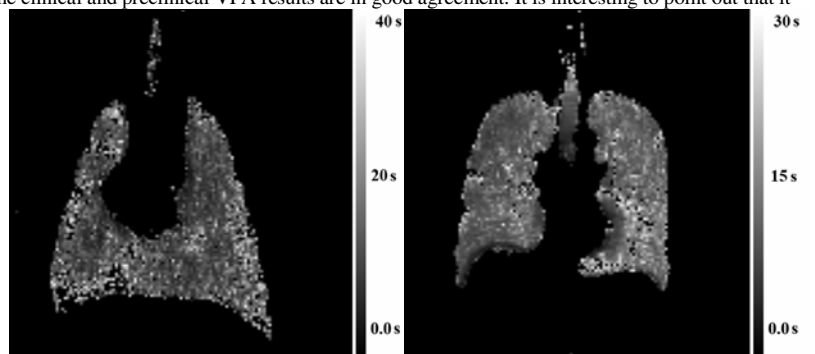


Fig 2. a) VFA T_1 map obtained for rat b) VFA T_1 map obtained for human subject